

again mechanistic complications in the ethyl benzene mechanism can easily be made responsible for the laser schlieren observations. Fast benzyl fragmentation with H formation and a competition with benzyl + H  $\rightarrow$  toluene combination, as well as other reactions, complicate the situation. Since benzyl fragmentation is not understood in detail (and we are far from this at present), the laser schlieren experiments do not appear direct enough to allow for a unique analysis of the complicated mechanism.

(xi) The present work does not give much insight into the later reactions governing final product formation such as provided to

- (58) Warnatz, J. In *Chemistry of Combustion Reactions*, Gardiner Jr., W. C., Ed.; Springer: New York, 1984.  
 (59) Roth, P.; Just, T. *Ber. Bunsenges. Phys. Chem.* **1975**, *79*, 682.  
 (60) Trenwith, A. B. *J. Chem. Soc., Faraday Trans. 2* **1986**, *82*, 457.  
 (61) Dempster, A. B.; Powell, D. B.; Sheppard, N. *Spectrochim. Acta* **1975**, *31A*, 245.  
 (62) Hitchcock, A. P.; Lapos, J. D. *J. Mol. Spectrosc.* **1975**, *54*, 223.  
 (63) Rudolph, H. D.; Dreizler, H.; Jäschke, A.; Wending, P. *Z. Naturforsch.* **1967**, *22a*, 940.  
 (64) Lutoshkin, V. J.; Kotorlenko, L. A.; Krugljak, Y. A. *Teor. Eksp. Khim* **1972**, *8*, 542.  
 (65) Ripoché, J. *Spectrochim. Acta* **1967**, *23A*, 1003.  
 (66) Grajcar, L.; Leach, S. J. *Chim. Phys.* **1964**, *61*, 1523.  
 (67) Varsanyi, G. *Assignments of 700 Benzene Derivatives*; Akademiai Kiadó: Budapest, 1973.  
 (68) Scip, R.; Schultz, G.; Hargittai, I.; Szabo, Z. G. *Z. Naturforsch.* **1977**, *32a*, 1178.  
 (69) Pang, F.; Boggs, J. E.; Pulay, P.; Forqarasi, G. *J. Mol. Struct.* **1980**, *66*, 281.  
 (70) Rossi, M.; Golden, D. M. *J. Am. Chem. Soc.* **1979**, *101*, 1230.  
 (71) Stull, D. R.; Westrum, E. F.; Sinke, G. G. *The Chemical Thermodynamics of Organic Compounds*; Wiley: New York, 1969.

a greater extent by mass spectrometry<sup>14,15</sup> and single-pulse shock experiments.<sup>8</sup> There are only two points to be raised here. The mechanism of ref 8 involves formation of benzyl and methylphenyl isomers. The latter are assumed to be much less stable than benzyl radicals. The estimated decomposition rates of methylphenyl are close to the present benzyl decomposition rates. This may suggest that there is essentially only one C<sub>7</sub>H<sub>7</sub> species involved. One may also argue that the experiments are completely insensitive to reaction 1, because of the fast recombination H + benzyl, such that reaction 2 dominates the overall reaction. However, in the presence of a fast benzyl consumption by other processes this argument can be ruled out on the basis of the present mechanistic modelling. Clearly, the fragmentation of benzyl provides the key for a further understanding of the system.

In summary one may state that the comparison of thermal and photochemical dissociation rates of toluene now presents a clear picture of the primary bond fission process. There appears to be clear indication of dominant C-H bond fission with well-established specific and thermally averaged rate constants. More work needs to be done in order to understand details of the fragmentation of benzyl radicals.

**Acknowledgment.** Financial support of this work by the Deutsche Forschungsgemeinschaft as well as calculational help by P. Borrell and collaboration with L. Lindemann on laser experiments are gratefully acknowledged.

**Registry No.** C<sub>7</sub>H<sub>8</sub>, 108-88-3; C<sub>7</sub>H<sub>7</sub>, 2154-56-5; PhCH<sub>2</sub>CH<sub>2</sub>Ph, 103-29-7; H, 12385-13-6; PhCHCH<sub>2</sub>Ph, 36877-87-9; Ph, 2396-01-2; PhPh, 92-52-4; C<sub>2</sub>H<sub>6</sub>, 74-84-0; CH<sub>3</sub>, 2229-07-4.

## Thermal Decomposition of Ethylbenzene, Styrene, and Bromophenylethane: UV Absorption Study in Shock Waves

W. Müller-Markgraf and J. Troe\*

*Institut für Physikalische Chemie der Universität Göttingen, Tammannstrasse 6, D-3400 Göttingen, West Germany (Received: September 9, 1987; In Final Form: February 17, 1988)*

Shock wave studies of the pyrolysis of ethylbenzene, isopropylbenzene, *tert*-butylbenzene, styrene, and 1-bromo-1-phenylethane were performed using UV molecular absorption spectroscopy. By extensive spectral studies over the range 190–330 nm the overlapping absorption continua could be separated. Key observations in ethylbenzene pyrolysis were the dominance of a primary C–C bond split, the comparably fast fragmentation of benzyl radicals in agreement with observations from other benzyl sources, and the evidence for nonnegligible styrene formation. The following rate constants were derived: ethylbenzene  $\rightarrow$  CH<sub>3</sub> + benzyl,  $k_1 = 10^{15.55} \exp(-306.7 \text{ kJ mol}^{-1}/RT) \text{ s}^{-1}$ ; styrene  $\rightarrow$  benzene + acetylene,  $k_{15} = 10^{11.2} \exp(-244.5 \text{ kJ mol}^{-1}/RT) \text{ s}^{-1}$ ; 1-bromo-1-phenylethane  $\rightarrow$  HBr + styrene,  $k_{22} = 10^{12.5} \exp(-160 \text{ kJ mol}^{-1}/RT) \text{ s}^{-1}$ ; benzyl fragmentation rates were identical with results from toluene, benzyl iodide, benzyl chloride, and other benzyl precursors. There is evidence for a dominant C–C bond split in isopropylbenzene and *tert*-butylbenzene pyrolysis as well.

### Introduction

The pyrolysis of aromatic hydrocarbons has been studied extensively at moderate temperatures and the derived mechanisms are generally accepted today. Recent extensions of these investigations to high-temperature combustion conditions, however, have indicated a number of complications. Under these conditions fragmentations of radical species become fast enough to compete with radical recombination processes. As a consequence, the number of fast bimolecular reactions involving small radicals increases markedly and the mechanisms become more complex. In addition, dissociation processes can proceed on several channels. The described complications call for studies using all available analysis techniques. The various methods for following the reaction all have their advantages and limitations so that a series of complementary experiments is required. Recent studies of the

pyrolysis of toluene, for example, have involved shock waves with laser schlieren, densitometry,<sup>1</sup> time-of-flight mass spectrometry,<sup>1</sup> UV molecular absorption,<sup>2-6</sup> atomic resonance absorption,<sup>7-10</sup> and

(1) Pamidimukkala, K. M.; Kern, R. D.; Patel, M. R.; Wei, H. C.; Kiefer, J. H. *J. Phys. Chem.* **1987**, *91*, 2148.

(2) Astholz, D. C.; Durant, J.; Troe, J. *Symp. (Int.) Combust., (Proc.)*, **18th** **1981**, 885.

(3) Astholz, D. C.; Troe, J. *J. Chem. Soc., Faraday Trans. 2* **1982**, *78*, 1413.

(4) Brouwer, L.; Müller-Markgraf, W.; Troe, J. *Symp. (Int.) Combust., (Proc.)*, **20th** **1984**, 799.

(5) Müller-Markgraf, W.; Troe, J. *Symp. (Int.) Combust., (Proc.)*, **21st** **1986**, 815.

(6) Brouwer, L.; Müller-Markgraf, W.; Troe, J. *J. Phys. Chem.*, preceding paper in this issue.

(7) Rao, V. S.; Skinner, G. B. *J. Phys. Chem.* **1984**, *88*, 4362.

single-pulse<sup>1,11</sup> techniques. Although these experiments still are interpreted in a rather controversial manner,<sup>1,5,6</sup> the key role of the benzyl radicals and their secondary reaction behavior has now been clearly identified.<sup>5,6</sup>

In the light of the new information on benzyl high-temperature reactions, the thermal dissociation of ethylbenzene in shock waves has to be reconsidered carefully. Moderate temperature studies of ethylbenzene dissociation have indicated dominant C–C bond fission<sup>12,13</sup>



Using UV molecular absorption spectroscopy we have extended such measurements to shock wave conditions.<sup>4,14</sup> Attributing the appearing UV absorptions to benzyl and styrene spectra, we obtained surprisingly small benzyl yields. This interpretation was done on the basis of benzyl absorption coefficients derived earlier from toluene dissociation and a calibration of styrene high-temperature absorption coefficients. Hence, a dominant C–H bond fission was postulated. However, this conclusion was disputed by recent laser schlieren,<sup>15</sup> atomic resonance absorption,<sup>16</sup> and single-pulse<sup>17,18</sup> shock wave experiments, as well as VLPP<sup>12,17</sup> and laser pyrolysis<sup>19</sup> studies. The use of an incorrect absorption coefficient was finally identified<sup>5,6</sup> as the error source. However, more detailed studies of benzyl properties in the pyrolysis of toluene and other benzyl precursors have, in addition, revealed unexpectedly fast rates of consumption of benzyl radicals.<sup>5,6,20</sup> As a matter of fact, our belief in the generally assumed large thermal stability of benzyl radicals was the basic reason for the earlier misinterpretations of UV molecular absorption experiments on toluene and ethylbenzene pyrolysis.

In view of the recent results on benzyl high-temperature kinetics and spectrum, a new shock wave study of ethylbenzene pyrolysis using UV molecular absorption detection appeared necessary. In spite of the overlap of continuous absorption spectra of several species involved, this technique can directly measure the concentrations of the parent molecules and the primary fragment radicals, whereas smaller fragments formed in later stages contribute to the near-UV spectra to a much smaller extent. This technique, therefore, allows for specific measurements "close to the primary steps" of the mechanism. The very sensitive hydrogen atom resonance absorption spectroscopy, on the other hand, can be influenced by H formation from a large group of secondary fragmentations. Indeed, the results on benzyl fragmentation in ethylbenzene pyrolysis using this technique<sup>16</sup> differ strongly from our molecular absorption results.<sup>5,6</sup> Therefore, as for toluene pyrolysis, a joint effort using all available complementary analysis techniques is required.

As in the case of toluene dissociation,<sup>6</sup> it should be emphasized that thermal dissociation experiments of ethylbenzene, as well as of benzyl radicals, should also be compared with collision-free laser-induced dissociation studies. Alternative explanations of the complicated thermal dissociation experiments can find a clear answer by such complementary experiments. Such experiments are under way in our laboratory.<sup>21</sup>

(8) Rao, V. S.; Skinner, G. B. submitted for publication in *J. Phys. Chem.*

(9) Frank, P.; Just, T. Poster presented at 21st Symposium (International) on Combustion, Munich, 1986.

(10) Braun-Unkhoff, M.; Frank, P.; Just, T. CEC Combustion Workshop, Abingdon, UK, Jan. 1987.

(11) Colket, M. B.; Seery, D. J. Poster presented at 20th Symposium (International) on Combustion, Ann Arbor, MI, 1984.

(12) Robaugh, D. A.; Stein, S. E. *Int. J. Chem. Kinet.* **1981**, *13*, 445.

(13) Davis, H. G. *Int. J. Chem. Kinet.* **1983**, *15*, 469.

(14) Brouwer, L.; Müller-Markgraf, W.; Troe, J. *Ber. Bunsenges. Phys. Chem.* **1983**, *87*, 1031.

(15) Mizerka, L. J.; Kiefer, J. H. *Int. J. Chem. Kinet.* **1986**, *18*, 363.

(16) Rao, V. S.; Skinner, G. B. *Symp. (Int.) Combust., (Proc.), 21st 1986*, 809.

(17) Robaugh, D. A.; Tsang, W.; Fahr, A.; Stein, S. E. *Ber. Bunsenges. Phys. Chem.* **1986**, *90*, 77.

(18) Pamidimukkala, K. M.; Kern, R. D. *Int. J. Chem. Kinet.* **1986**, *18*, 1341.

(19) Gonzalez, A. C.; Larson, C. W.; McMillen, D. F.; Golden, D. M. *An. Asoc. Quim. Argent.* **1985**, *73*(2), 141.

(20) Müller-Markgraf, W.; Troe, J. *J. Phys. Chem.*, first of three papers in this issue.

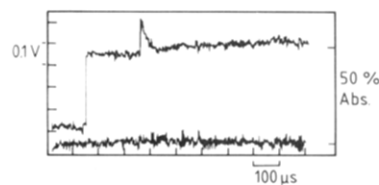


**Figure 1.** Absorption-time profile at  $\lambda = 190$  nm during the pyrolysis of ethylbenzene in shock waves. First step: absorbing "hot" ethylbenzene in the incident shock wave. Conditions of reflected shock:  $T = 1465$  K,  $[\text{ethylbenzene}]_{t=0} = 1.8 \times 10^{-9}$  mol  $\text{cm}^{-3}$ ,  $[\text{Ar}] = 3.08 \times 10^{-5}$  mol  $\text{cm}^{-3}$ ; the lower trace indicates the base line from the pulsed light source.

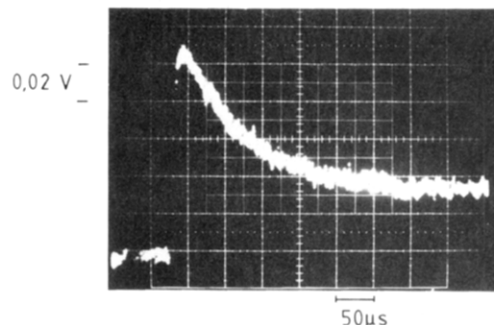


**Figure 2.** Absorption-time profile at  $\lambda = 270$  nm during the pyrolysis of ethylbenzene (reflected shock:  $T = 1575$  K,  $[\text{ethylbenzene}]_{t=0} = 3.04 \times 10^{-9}$  mol  $\text{cm}^{-3}$ ,  $[\text{Ar}] = 2.0 \times 10^{-5}$  mol  $\text{cm}^{-3}$ ).

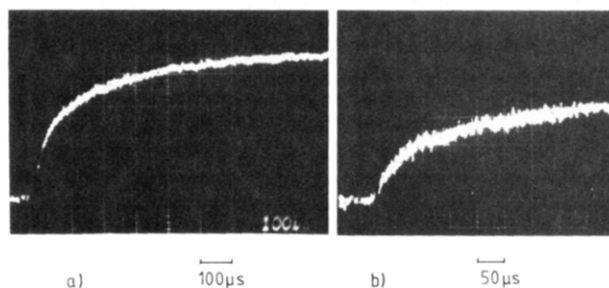


**Figure 3.** Absorption-time profiles during the pyrolysis of ethylbenzene: (a)  $\lambda = 260$  nm,  $T = 1325$  K,  $[\text{ethylbenzene}]_{t=0} = 5.83 \times 10^{-9}$  mol  $\text{cm}^{-3}$ ,  $[\text{Ar}] = 8.8 \times 10^{-5}$  mol  $\text{cm}^{-3}$ ; (b)  $\lambda = 270$  nm,  $T = 1335$  K,  $[\text{ethylbenzene}]_{t=0} = 3.75 \times 10^{-9}$  mol  $\text{cm}^{-3}$ ,  $[\text{Ar}] = 2.5 \times 10^{-5}$  mol  $\text{cm}^{-3}$ .

Besides the role of benzyl radicals in the high-temperature pyrolysis, the amount of styrene formation has to be reinvestigated. Styrene formation can be followed by UV molecular absorption spectroscopy. However, again the spectrum has to be separated most carefully from continua of other absorbing species like benzyl and "benzyl fragments" (as characterized in our earlier benzyl studies<sup>5</sup>). There are several pathways for the formation of styrene. Styrene yields, therefore, may serve as an indicator for the understanding of the general mechanism. With most other techniques, styrene yields were measured by final product analysis. Hence, an in situ detection of styrene appears also desirable.

#### Experimental Technique and Measured Absorption Signals

Our experimental technique has been described before<sup>2-6</sup> and will only in part be characterized. Measurements were done in incident and reflected shock waves. Absorption measurements covered the spectral range 190–330 nm. Initial concentrations of the reactants generally were between 10 and 100 ppm in Ar, and argon concentrations typically were around  $3.0 \times 10^{-5}$  mol  $\text{cm}^{-3}$ .

#### Absorption Signals in Ethylbenzene Pyrolysis

In order to detect dominant absorption from the parent molecule ethylbenzene, short absorption wavelengths had to be applied. A typical oscillogram is given in Figure 1, showing the disappearance of the parent molecular absorption at 190 nm. There is a strong

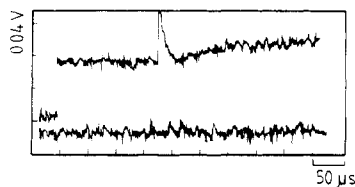


**Figure 4.** Absorption-time profile at  $\lambda = 210$  nm during the pyrolysis of styrene. Reflected shock:  $T = 2015$  K,  $([\text{styrene}]/[\text{Ar}])_{t=0} = 160$  ppm,  $[\text{styrene}]_{t=0} = 3.4 \times 10^{-9}$  mol  $\text{cm}^{-3}$ ,  $[\text{Ar}] = 3.4 \times 10^{-5}$  mol  $\text{cm}^{-3}$ .

residual absorption at this wavelength which, as later investigations indicate, has to be attributed to an overlap of toluene, styrene, and benzyl fragment spectra.

Measurements at longer observation wavelengths show different absorption profiles. Figure 2 reproduces an oscillogram recorded at 270 nm under only slightly higher temperature conditions. At this wavelength, there is no high-temperature absorption from the parent molecule,<sup>14</sup> and the spectrum is attributed to the rapid formation of benzyl radicals and their slightly slower consumption. The residual absorption must contain benzyl fragment contributions, such as observed in separate benzyl studies, and styrene contributions.

We have systematically studied the short- and long-wavelength absorption profiles as a function of temperature and parent molecule concentration. By variation of the observation wavelengths, a careful analysis of the various spectral contributions was possible. Figure 3 shows two experiments under similar conditions but with observations at 260 and 270 nm. There are fine but characteristic differences; e.g., there is a "kink" in the trace at 270 nm after about 100  $\mu\text{s}$ , which is not an artifact but a result of the overlap of several components.

The modelling of the absorption-time profile at different wavelengths and conditions required a separation of the contributing spectral components. This was possible since, at least in part, separate studies of these components could be undertaken. For benzyl radicals, we earlier studied a variety of precursor molecules which have all now led to a consistent spectrum and to consistent kinetic properties. Therefore, genuine benzyl contributions can clearly be identified. Similarly, the spectral properties of benzyl fragments are well characterized now. In the present system, besides benzyl and benzyl fragments there are additional spectral components which we tentatively attribute to styrene. For this reason a comparison with genuine styrene properties was required.

#### Absorption Signals in Styrene Pyrolysis

Styrene is a particularly stable molecule which can be produced in ethylbenzene pyrolysis. Spectral and kinetic properties of this molecule were investigated in experiments with about 100 ppm styrene in argon. At the temperatures of benzyl and ethylbenzene decomposition, no styrene dissociation was observed so that the high-temperature spectrum could be studied without any kinetic complications. Around 2000 K, styrene decomposes on a 100- $\mu\text{s}$  time scale. Figure 4 shows a typical absorption-time profile at 210 nm. The dominant parent absorption disappears, but a considerable residual absorption is formed. The spectrum of the "styrene fragments" was recorded and calibrated at various wavelengths. Final spectra and spectra at the minimum of the absorption-time curve differed in shape. The spectrum at the minimum appeared to contain an important contribution of hot benzene absorption, whereas the final spectrum corresponds to benzene fragments.

#### Absorption Signals in 1-Bromo-1-phenylethane Pyrolysis

The pyrolysis of 1-bromo-1-phenylethane yields 1-phenylethyl radicals with a spectrum fairly similar to that of benzyl radicals.<sup>21</sup> In order to investigate possible formation of 1-phenylethyl radicals in ethylbenzene pyrolysis, we tried to produce these radicals via the pyrolysis of 1-bromo-1-phenylethane. Figure 5 shows the absorption profiles observed at low and high temperatures. The molecule decomposes and a stable strongly absorbing molecule

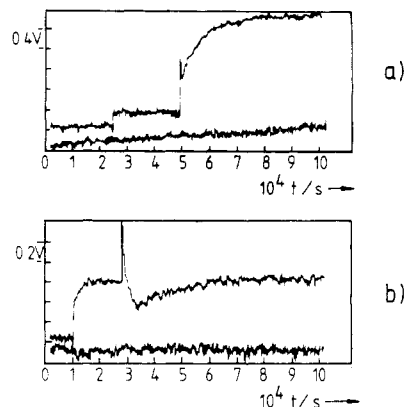


**Figure 5.** Absorption-time profiles during the thermal decomposition of 1-bromo-1-phenylethane (BrPhEt). (a)  $\lambda = 257.5$  nm; incident shock,  $T = 597$  K; reflected shock,  $T = 976$  K,  $[\text{BrPhEt}]_{t=0} = 7.8 \times 10^{-9}$  mol  $\text{cm}^{-3}$ ,  $[\text{Ar}] = 5.1 \times 10^{-5}$  mol  $\text{cm}^{-3}$ ; (b)  $\lambda = 245$  nm, incident shock,  $T = 1009$  K,  $[\text{Ar}] = 1.05 \times 10^{-5}$  mol  $\text{cm}^{-3}$ ,  $[\text{BrPhEt}]_{t=0} = 1.13 \times 10^{-9}$  mol  $\text{cm}^{-3}$ ; reflected shock,  $T = 1947$  K,  $[\text{styrene}]_{t=0} = 2.45 \times 10^{-9}$  mol  $\text{cm}^{-3}$ ,  $[\text{Ar}] = 2.28 \times 10^{-5}$  mol  $\text{cm}^{-3}$ .

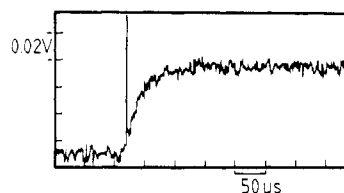
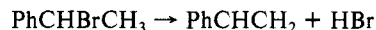


**Figure 6.** Absorption-time profile at  $\lambda = 270$  nm of product formation in isopropylbenzene decomposition.  $T = 1340$  K,  $([\text{isopropylbenzene}]/[\text{Ar}])_{t=0} = 150$  ppm,  $[\text{Ar}] = 3.0 \times 10^{-5}$  mol  $\text{cm}^{-3}$ ; schlieren signal at the arrival of the reflected shock.

is obtained which easily is identified as styrene. In the low-temperature experiment, styrene is formed behind the reflected wave; in the high-temperature experiment, it is formed behind the incident wave and decomposes behind the reflected wave. Apparently styrene here is formed via the elimination



The styrene signals from this styrene precursor were in all details identical with genuine styrene experiments. No information on phenylethyl radicals was obtained in this way. However, the high-temperature spectra of these radicals are now known from laser photolysis experiments.<sup>21</sup>

#### Absorption Signals in the Pyrolysis of Isopropylbenzene, *tert*-Butylstyrene, and $\alpha$ -Methylstyrene

In earlier work<sup>4</sup> we also investigated the pyrolysis of isopropylbenzene and *tert*-butylbenzene by the UV molecular absorption technique. In view of the new information on benzyl, these studies had to be repeated. Figure 6 shows the formation of a stable product absorption at 270 nm in the pyrolysis of isopropylbenzene. The spectral features of this spectrum were carefully analyzed, allowing for an identification with the spectrum of styrene (see below). On the other hand *tert*-butylbenzene pyrolysis led to a product spectrum, which was slightly less stable than styrene but which, by comparison with genuine  $\alpha$ -methylstyrene, could be attributed to  $\alpha$ -methylstyrene (see below).

#### Separation of Overlapping Absorption Spectra

The recorded absorption-time profiles described in the previous section have to be separated into the contributions from different species. These are the parent molecules, benzyl radicals, benzyl fragments, and styrene. Only at very high temperatures ( $T \gtrsim 2000$  K), where styrene decomposes, spectra from benzene and benzene fragments have to be taken into account. (For the *tert*-butylbenzene system,  $\alpha$ -methylstyrene is considered.) The spectrum of phenylethyl radicals is known from laser photolysis to be similar to that of benzyl radicals. However, as described below, this spectrum was not taken into consideration any longer.

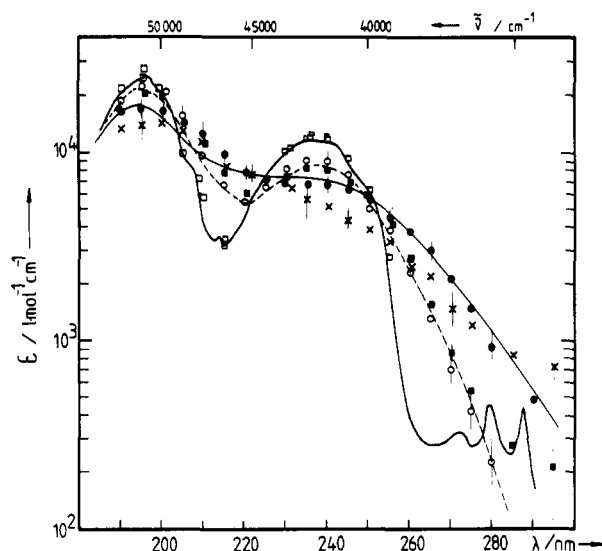


**Figure 7.** Styrene absorption spectrum at (—)  $T = 300$  K (Cary 17 D spectrometer); (□)  $T = 300$  K (shock tube); (○)  $T = 820$  K with (---) modified Sulzer-Wieland fit<sup>22</sup> for interpolation; (■)  $T = 1050$  K; (●)  $T = 1500$  K with (—) modified Sulzer-Wieland fit,<sup>22</sup> (×)  $T = 2050$  K.

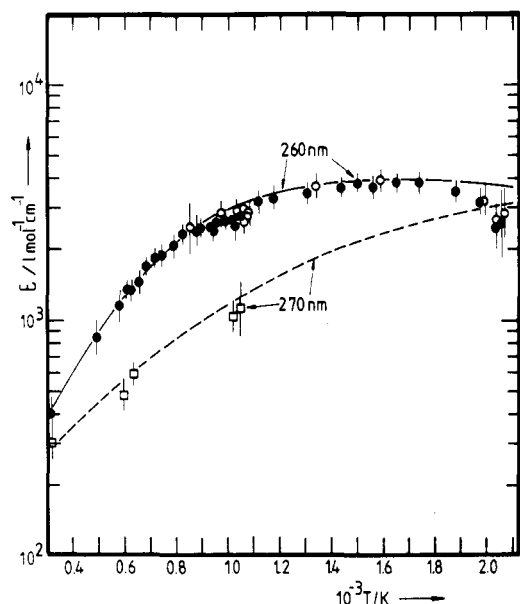


**Figure 8.** Temperature dependence of the absorption coefficient of styrene at  $\lambda = 260$  and  $270$  nm. (—, ---) Numerical representation using modified Sulzer-Wieland formalism<sup>22</sup> for convenient interpolation, see Figure 7.  $\lambda = 260$  nm: (●) genuine styrene, (○) styrene from 1-bromo-1-phenyl.  $\lambda = 270$  nm: (□) genuine styrene.

The different spectral components and their kinetic features under separate conditions were identified separately as far as possible so that absorption coefficients for the full spectrum were known from independent determination. Complete fits to the ethylbenzene system, such as described below, confirm these earlier studies. In the following, at first we give a preliminary analysis of the overlapping spectra identifying the global kinetic features in an approximate way. A fine tuning is performed afterwards by a refined parameter fit on the basis of detailed kinetic modelling.

Hot toluene, benzyl radical, and benzyl fragments spectra have been documented in detail in ref 6 and are not shown here. It should, however, be emphasized that final fit values of benzyl radical absorption coefficients from ethylbenzene decomposition agree perfectly with the independent earlier determinations. These points are included in our earlier articles.<sup>5,6</sup> The present determinations of hot UV absorption spectra of styrene are shown in Figure 7. The results from genuine styrene experiments agree quantitatively with values from the pyrolysis of 1-bromo-1-

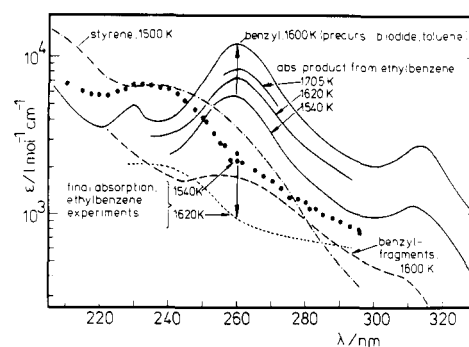


**Figure 9.** Change of "apparent absorption coefficients" of products in ethylbenzene pyrolysis with temperature (for a detailed description of the figure, see text); (●) spectrum of the final absorption in ethylbenzene thermal decomposition experiments of ref 14.

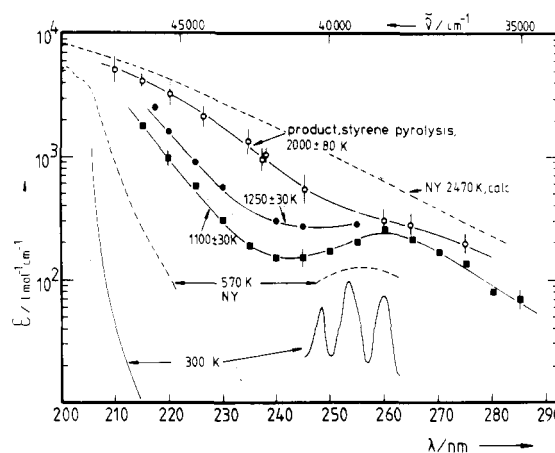


**Figure 10.** Absorption spectra of benzene in comparison to measured product absorptions (○) in styrene pyrolysis; (--- NY) measured (570 K) and calculated (570 and 2470 K) hot spectra after laser excitation from ref 33; (●, ■) measured in shock waves, from ref 34.

phenylethane as demonstrated in Figure 8. The dominant pathway (2) of pyrolysis of the latter substance via HBr elimination is thus confirmed.

Figure 9 compares benzyl radical, benzyl fragment, and styrene spectra with spectra of reaction products such as recorded in the ethylbenzene pyrolysis. These spectra are "calibrated" as if one ethylbenzene would give one product. The first absorbing reaction product, demonstrated in Figures 2 and 3, has a spectrum which according to Figure 9 looks very similar to genuine benzyl. However, the "apparent absorption coefficient" is strongly temperature dependent. Identifying this species with benzyl radicals, consequently, an increasing benzyl yield with increasing temperature is obtained. The final fragment spectrum has a much smaller apparent absorption coefficient (see Figure 9). The shape of the spectrum is neither that of pure benzyl fragments nor of pure styrene, but can be constructed from an overlap of these two components. According to Figure 9, the yield of this final fragment spectrum of ethylbenzene pyrolysis decreases with increasing temperature. In analyzing the final spectra, one should take into consideration the time scale (up to 1 ms) of the present experiments. Since ethylbenzene decays about 100 times faster and benzyl about 10 times faster than toluene, some "missing absorption" can be attributed to a transient formation of the relatively stable toluene which absorbs only weakly around 240–280 nm.<sup>22</sup> Nevertheless, hot toluene absorption can contribute to the residual absorption at 190 nm as shown in Figure 1.

Figure 9 demonstrates the major contributions to the overlapping spectra recorded in ethylbenzene decomposition. At shorter wavelengths, in addition there are parent ethylbenzene

(22) Astholz, D. C.; Brouwer, L.; Troe, J. *Ber. Bunsenges. Phys. Chem.* **1981**, *85*, 559.

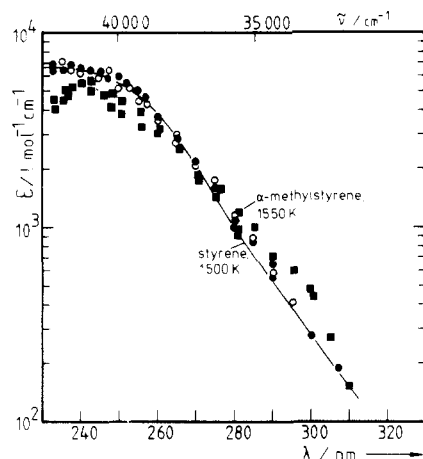


**Figure 11.** Product spectra from the pyrolysis of isopropylbenzene (●) and *tert*-butylbenzene (○) at  $T = 1330$  K, compared with styrene (—) at  $T = 1500$  K and  $\alpha$ -methylstyrene (■) at  $T = 1550$  K.

and intermediate toluene spectra.

We have also analyzed fragment spectra in styrene pyrolysis for much higher temperatures than applied in ethylbenzene pyrolysis. Two components were identified, one intermediate spectrum at the minimum of the absorption-time profiles in Figures 4 and 5, and one final spectrum at the end of the shown traces. Figure 10 compares the intermediate component (evaluated assuming one styrene  $\rightarrow$  one intermediate) with hot benzene spectra. Our observations would be consistent with the assumption of a 1:1 conversion of styrene into benzene + acetylene (see below). The spectra of final fragments from styrene pyrolysis essentially agree with those obtained from benzene as well as from benzyl fragmentation. However, since there is surely an overlap from several species formed late in the reaction, we did not further try to split up the final spectra into their components.

Figure 11 compares product spectra from the pyrolysis of isopropylbenzene and *tert*-butylbenzene with styrene. The agreement indicates essentially a 1:1 conversion. However, for *tert*-butylbenzene the formation of  $\alpha$ -methylstyrene also has to be discussed (see below). Figure 11 includes a hot UV spectrum of genuine  $\alpha$ -methylstyrene which is close but not identical with the genuine styrene spectrum. No distinction of the products can be made for *tert*-butylbenzene pyrolysis.

#### Analysis of the Mechanism of Ethylbenzene Pyrolysis

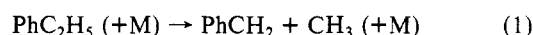
In the previous section, the absorption continua contributing to the observed absorption-time profiles have been described. In the following, the kinetic properties of the present experiments are analyzed. In spite of the low ethylbenzene concentrations applied, always a mechanism of primary and secondary reaction steps had to be taken into account. The absorption signals at short wavelengths (190 nm) and at long wavelengths (240–280 nm) depended on these reactions with different sensitivities. Surely, it would not have been possible to extract from our experiments a great number of rate parameters and absorption coefficients independently by a parameter-fitting procedure. However, with the knowledge of much of these data from separate previous studies such as our investigations of benzyl<sup>5,20</sup> and of toluene<sup>5,6</sup> properties, a limited number of new parameters now could be fitted with confidence. The misinterpretation of our earlier ethylbenzene experiments<sup>14</sup> was due to the input of inadequate toluene and benzyl data.

In the present work the following quantities can be extracted from the recorded UV absorption spectra: the rate of primary C–C bond fission in ethylbenzene, the rate of benzyl “fragmentation” and the benzyl radical absorption coefficient (in comparison to similar information from other benzyl systems), an upper limit for the rate of primary C–H bond fission in ethylbenzene, and an in situ determination of the styrene yields after the first stage of reaction. These data follow from a complex mechanism, but the sensitivity of the observables with respect to

these data was tested and found large enough for unique conclusions.

The relevant mechanism involves the primary bond fission of ethylbenzene, bimolecular attack of the parent molecule by radicals, the complete toluene and benzyl mechanisms analyzed earlier, and reactions forming relatively stable end products like styrene. We do not consider all details of the final degradation into small fragments which may influence final product distributions.

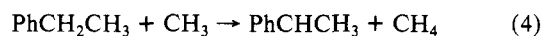
Our reaction mechanism starts with a dominant primary C–C bond fission ( $\text{Ph} = \text{C}_6\text{H}_5$ )



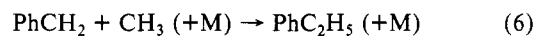
We also try to derive an upper limit of the C–H bond split followed by phenylethyl,  $\text{PhC}_2\text{H}_5$ , fragmentation, i.e., the “direct styrene mechanism”



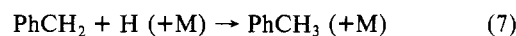
There is rapid attack of the parent molecule by radicals via



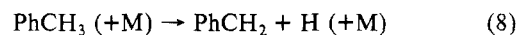
where H atoms are generated via phenylethyl fragmentation (3). The benzyl radicals  $\text{PhCH}_2$  primarily formed may either combine with  $\text{CH}_3$



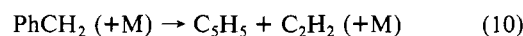
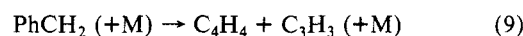
reconstituting the parent molecule or combine with H to lead over into the toluene system



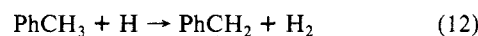
Further important steps are the reverse toluene fragmentation



benzyl fragmentations



and subsequent fragmentations of benzyl fragments liberating more hydrogen atoms, as well as radical reactions attacking toluene such as



These reactions all are also important in the toluene and benzyl radical systems. (For further details of this mechanism, especially reactions of smaller fragments, see ref 18.) The precursor for styrene formation is the dissociation of phenylethyl in reaction 3; here the “bimolecular styrene mechanism” (4), (5), and (3) apparently dominates over the direct styrene mechanism (2) and (3). As long as phenylethyl does not fragment via reaction 3, hydrogen abstraction by other radicals may also lead to styrene. Alternatively, styrene production will be intercepted by the reactions



proceeding via an excited ethylbenzene intermediate. Finally, benzyl radicals can also abstract H from ethylbenzene leading again into the toluene system via



Styrene dissociation sets in only at higher temperatures ( $T > 1700$  K) and is neglected in the present modelling.

We have simulated the observable absorption-time profiles of our work on the basis of the mechanism (1)–(14). The observed profiles are all well represented in this way; “later” processes from benzyl fragments or other smaller species turned out not to be too important for our observations. It should, however, be em-

TABLE I: Summary of Reactions and Kinetic Parameters in Ethylbenzene Pyrolysis<sup>a</sup>

	log <i>A</i>	<i>E</i> <sub>a</sub> /kJ mol <sup>-1</sup>	reference
1. PhCH <sub>2</sub> CH <sub>3</sub> → PhCH <sub>2</sub> + CH <sub>3</sub>	15.55	306.7	present work, 2 × 10 <sup>-5</sup> ≤ [Ar] ≤ 2.4 × 10 <sup>-4</sup> mol cm <sup>-3</sup>
2. PhCH <sub>2</sub> CH <sub>3</sub> → PhCHCH <sub>3</sub> + H	15.4	340.0	present work, estimated upper limit
3. PhCHCH <sub>3</sub> → PhCHCH <sub>2</sub> + H	13.5	212	estimated, 28
	15.9	217	estimated, 29
4. PhCH <sub>2</sub> CH <sub>3</sub> + CH <sub>3</sub> → PhCHCH <sub>3</sub> + CH <sub>4</sub>	12.4–12.6	0	30
5. PhCH <sub>2</sub> CH <sub>3</sub> + H → PhCHCH <sub>3</sub> + H <sub>2</sub>	<i>A</i> = 10 <sup>-4.1</sup> <i>T</i> <sup>5.5</sup>	1.4	estimated, 31
6. PhCH <sub>2</sub> + CH <sub>3</sub> → PhCH <sub>2</sub> CH <sub>3</sub>	12.4–12.7	0	estimated
7. PhCH <sub>2</sub> + H → PhCH <sub>3</sub>	13.9–14.2	0	6
8. PhCH <sub>3</sub> → PhCH <sub>2</sub> + H	15.3	369.1	5, 6; [Ar] ≈ 3 × 10 <sup>-5</sup> mol cm <sup>-3</sup>
9. PhCH <sub>2</sub> → C <sub>4</sub> H <sub>4</sub> + C <sub>3</sub> H <sub>3</sub>	15.3	349.6	5, 6; [Ar] ≈ 3 × 10 <sup>-5</sup> mol cm <sup>-3</sup>
10. PhCH <sub>2</sub> → C <sub>3</sub> H <sub>3</sub> + C <sub>2</sub> H <sub>2</sub>	10.22	187	5, 6; [Ar] ≈ 3 × 10 <sup>-5</sup> mol cm <sup>-3</sup>
11. PhCH <sub>3</sub> + CH <sub>3</sub> → PhCH <sub>2</sub> + CH <sub>4</sub>	12.5	0	estimated, 30
12. PhCH <sub>3</sub> + H → PhCH <sub>2</sub> + H <sub>2</sub>	<i>A</i> = 10 <sup>-4.12</sup> <i>T</i> <sup>5.5</sup>	1.422	7
13. PhCHCH <sub>3</sub> + H → PhCH <sub>2</sub> + CH <sub>3</sub>	treated as recombination/bond fission with log <i>k</i> <sub>rec</sub> ≈ 14.2 and decomposition as reaction 1		
14. PhCH <sub>2</sub> + PhCH <sub>2</sub> CH <sub>3</sub> → PhCH <sub>3</sub> + PhCHCH <sub>3</sub>	12	0	estimated, 19
15. PhCHCH <sub>2</sub> → C <sub>6</sub> H <sub>6</sub> + C <sub>2</sub> H <sub>2</sub>	11.2	244.5	present work, [Ar] ≈ 3 × 10 <sup>-5</sup> mol cm <sup>-3</sup>
16. C <sub>6</sub> H <sub>6</sub> + C <sub>2</sub> H <sub>2</sub> → PhCHCH <sub>2</sub>	<i>RTk</i> <sub>15</sub> / <i>K</i> <sub>p</sub> with <i>K</i> <sub>p</sub> = 10 <sup>6.50</sup> exp(-19476/ <i>T</i> ) atm		
17. C <sub>6</sub> H <sub>6</sub> → C <sub>4</sub> H <sub>4</sub> + C <sub>2</sub> H <sub>2</sub>	14.11	368.2	25
18. C <sub>6</sub> H <sub>6</sub> → Ph + H	15.7	227.2	26
	16.76	244.35	26, <i>k</i> <sub>∞</sub>
19. Ph → C <sub>4</sub> H <sub>3</sub> + C <sub>2</sub> H <sub>2</sub>	15.08	343	25, 10
20. C <sub>4</sub> H <sub>3</sub> → C <sub>4</sub> H <sub>2</sub> + H	11.3	213.4	25
21. C <sub>6</sub> H <sub>5</sub> + H → C <sub>6</sub> H <sub>6</sub>	13.5	0	estimated, 10
22. PhCHBrCH <sub>3</sub> → PhCHCH <sub>2</sub> + HBr	12.5	160	present work
23. PhCH(CH <sub>3</sub> ) <sub>2</sub> → PhCHCH <sub>3</sub> + CH <sub>3</sub>	15.8	298.3	12, <i>k</i> <sub>∞</sub>
24. PhC(CH <sub>3</sub> ) <sub>3</sub> → PhC(CH <sub>3</sub> ) <sub>2</sub> + CH <sub>3</sub>	15.9	289.1	12, <i>k</i> <sub>∞</sub>
25. PhC(CH <sub>3</sub> ) <sub>2</sub> → PhCCH <sub>3</sub> CH <sub>2</sub> + H	as reaction 3		

<sup>a</sup>Representation  $k = A \exp(-E_a/RT)$ ; *A* in s<sup>-1</sup> or cm<sup>3</sup> mol<sup>-1</sup> s<sup>-1</sup>, Ph = C<sub>6</sub>H<sub>5</sub>.

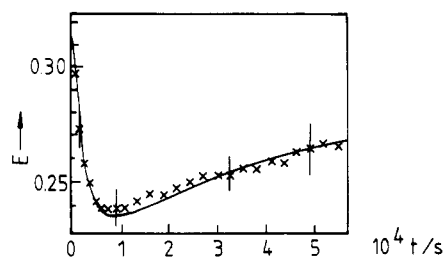


Figure 12. Simulation of the ethylbenzene pyrolysis experiment from Figure 1 at  $\lambda = 190$  nm: (x) experimental data, (—) model calculation.

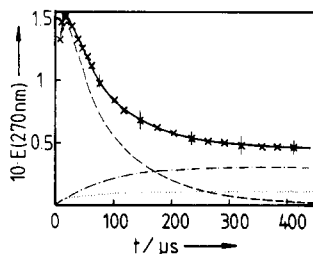


Figure 13. Simulation of the experiment from Figure 2: (x) experimental data; (—) calculated absorption  $E = \log(I_0/I)$  with contributions from benzyl (---), benzyl fragments (.....), and styrene (—·—·).

phasized that these omitted steps are of importance for final product yields as well as for the details of concentration profiles for small radicals such as H atoms.

Table I summarizes the rate parameters used in our present simulations. Figures 12–14 show the corresponding contributions to the absorption signals from Figures 1–3. The reproduction of the experimental signals is excellent, even in the finest details such as the “kink” in Figure 3b which is due to a fairly abrupt change in the benzyl rise. In addition to reactions 1–14, we have also made simulations including extended toluene–benzyl mechanisms like those discussed in ref 6. Figure 15 demonstrates the almost negligible influence of these additional reactions on the simulated absorption profiles near 260 nm. On the other hand, for a smaller initial concentration, Figure 15b simulates the effect of an important C–H bond split via reaction 2 ( $k_2/k_1 \approx 1.4:1$ ). The profiles

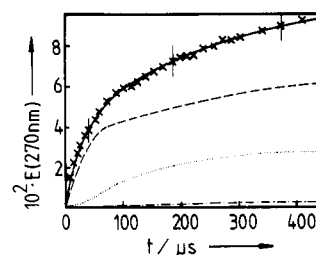


Figure 14. As in Figure 13, for the experiment from Figure 3.

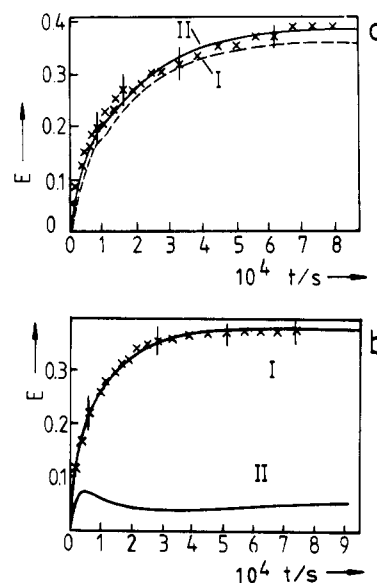
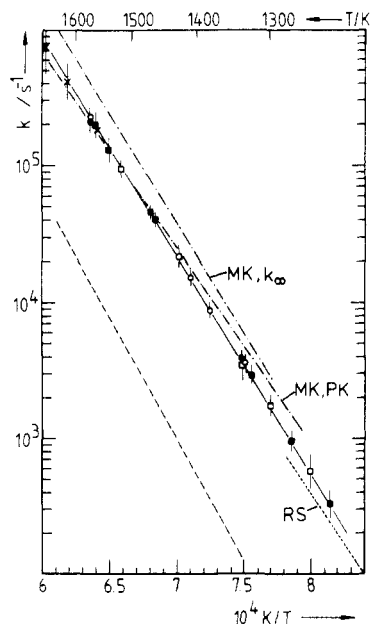


Figure 15. (a) Model calculations of observed absorption profiles in ethylbenzene pyrolysis, see text (I, “simple” mechanism from this work; II, mechanism including full set of reactions from ref 6; x, experimental profile, conditions  $T = 1335$  K,  $([\text{ethylbenzene}]/[\text{Ar}])_{t=0} = 260$  ppm,  $\lambda = 260$  nm,  $[\text{Ar}] = 3 \times 10^{-5}$  mol cm<sup>-3</sup>). (b) Influence of reaction 2 on the calculated absorption–time profiles; calculations with  $k_1 = 4.6 \times 10^4$  s<sup>-1</sup>,  $k_2 = 10^3$  s<sup>-1</sup> (I), or with  $k_1 = 4.6 \times 10^4$  s<sup>-1</sup>,  $k_2 = 6 \times 10^4$  s<sup>-1</sup> (II); (x) experimental profile at  $T = 1470$  K ( $[\text{ethylbenzene}]/[\text{Ar}]_{t=0} = 65$  ppm,  $\lambda = 260$  nm,  $[\text{Ar}] = 2 \times 10^{-4}$  mol cm<sup>-3</sup>).



**Figure 16.** First-order rate constants for reaction 1: (—) this work with  $([\text{ethylbenzene}]/[\text{Ar}])_{t=0} = 200$  ppm ( $\times$ ), 260 ppm ( $\circ$ ), 100 ppm ( $\bullet$ ), 65 ppm ( $\blacksquare$ ),  $\leq 35$  ppm ( $\square$ ), and  $2.0 \times 10^5 \leq [\text{Ar}] \leq 2.4 \times 10^{-4}$  mol cm $^{-3}$ ; (---) upper limit for reaction 2; MK = ref 15, PK = ref 18, RS = ref 12.

are quite different from the observations. In this way an upper limit for  $k_2/k_1$  of about 0.1 could be estimated.

The results of our simulations are as follows:

(i) Benzyl fragmentation rates  $k_9 + k_{10}$  and benzyl radical absorption coefficients are in good agreement with all other benzyl systems studied before. Therefore, we have included these benzyl results in the representations of ref 6 and 20 without showing them here.

(ii) The next independent result from this work is a verification of a dominant primary C–C bond fission (1) in agreement with other recent conclusions,<sup>12,13,15–19</sup> and an estimate of an upper limit of only 10% for the competing C–H bond split (2). This result supersedes our earlier incorrect interpretation of the absorption profiles.

(iii) Our new results on the primary dissociation rate of ethylbenzene, such as derived essentially from the early part of the benzyl radical appearance signals, do not differ too much from our old data, but now they are based on a consistent mechanistic interpretation. Figure 16 compares our results with recent measurements using other techniques. We do not confirm the low apparent activation energy from the laser schlieren studies of ref 15 which has been attributed to high-temperature falloff effects. As in the case of toluene pyrolysis, we have undertaken detailed falloff simulations ourselves,<sup>21</sup> going beyond simple RRKM modelling. Our experiments over the range  $2 \times 10^{-5} \leq [\text{Ar}] \leq 2.4 \times 10^{-4}$  mol cm $^{-3}$  did not indicate any appreciable pressure dependence of  $k_1$ . The derived Arrhenius expression of  $k_1$  is

$$k_1 = 10^{15.55 \pm 0.12} \exp(-306.7 (\pm 3) \text{ kJ mol}^{-1} / RT) \text{ s}^{-1}$$

at  $2.0 \times 10^{-5} \leq [\text{Ar}] \leq 2.4 \times 10^{-4}$  mol cm $^{-3}$  over the temperature range 1250–1680 K. Our falloff calculations for 1600 K and  $[\text{Ar}] \approx 5 \times 10^{-5}$  mol cm $^{-3}$  led to a falloff estimate  $k_1/k_\infty$  of about 0.59 with only weak temperature dependence of this factor. We, therefore, interpret the low activation energy of  $k_1$  from ref 15 as a mechanistic effect. As a matter of fact, the laser schlieren experiments were evaluated neglecting the rapid consumption of benzyl radicals and the similarly rapid coupling-in of the toluene system. The complexity of the total mechanism and the large number of possible H atom sources and sinks from the fragments also put some question marks on the recent H atomic resonance absorption studies of ethylbenzene and benzyl fragmentation from ref 16. Although in this work  $k_1$  was derived in fair agreement

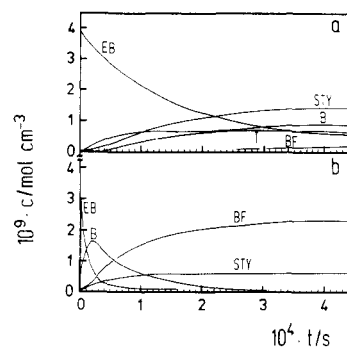


**Figure 17.** (a) Calculated concentration–time profiles for the experiment of Figure 3b. (b) As in Figure 17a, for the experiment of Figure 2. Abbreviations: EB = ethylbenzene, STY = styrene, B = benzyl, BF = benzyl fragments, T = toluene ( $\leq 2.4 \times 10^{-10}$  mol cm $^{-3}$  in Figure 17 b).

with the present results, very slow benzyl dissociation rates, in disagreement with our much more direct observations via benzyl spectra, were obtained. As for toluene dissociation, H atom profiles are sensitive to a much larger number of poorly understood reactions and, therefore, appear less uniquely interpretable than the present molecular absorption signals which are close to the initial stages of the reaction.

Our earlier conclusion of a 1:1 conversion of ethylbenzene into styrene was drawn on the basis of incomplete knowledge of the overlapping spectra. With the present information, this conclusion has to be revised. Figures 13–15 show that the absorption signals do not provide unique measurements of styrene concentrations. However, the benzyl radical and benzyl fragment components of the signals are fairly well-known now so that they can be subtracted. The remaining parts of the absorption signals are attributed to styrene. Evaluated with the measured temperature-dependent styrene absorption coefficients, full consistency with the model calculations is obtained. With the benzyl radical, benzyl fragment, and styrene absorption coefficients, Figures 13–15 can directly be converted into styrene concentration profiles. In order to facilitate the analysis, Figure 17a,b shows typical detailed concentration profiles resulting from our simulation. These profiles are fully consistent with the styrene absorption profiles in Figures 13–15. Our styrene yields are roughly consistent with the results from TOF,<sup>18</sup> VLPP,<sup>17</sup> and laser pyrolysis<sup>19</sup> studies. The scavenger inhibition studies by laser pyrolysis confirm the unimportance of the direct styrene mechanism (2) and (3) as compared to the bimolecular styrene mechanism (4), (5), and (3). There is apparently an increase of styrene yields with increasing temperature before the yield decreases again at higher temperatures when styrene dissociation sets in. The maximum styrene yields obtainable, of course, depend on temperature and on ethylbenzene concentration. Therefore, the various experimental conditions cannot be compared without thorough inspection of the mechanism. Under our conditions we estimate maximum obtainable styrene yields (relative to the initial ethylbenzene) of the order of 50%. Maximum final yields of 15% were found in laser pyrolysis,<sup>19</sup> 25% in TOF experiments,<sup>18</sup> and 18% in single-pulse experiments<sup>17</sup> for a variety of conditions.

#### Decomposition of Styrene and 1-Bromo-1-phenylethane

Under conditions of our studies of ethylbenzene pyrolysis, styrene is a stable product. Separate studies of styrene pyrolysis from genuine styrene and 1-bromo-1-phenylethane systems allowed us to derive styrene primary decomposition rates. Again the overlapping absorption spectra of the parent styrene molecules, of a primary product identified as benzene, and of “final fragments” had to be carefully separated.

On the basis of photodissociation studies of styrene and of cyclooctatetraene,<sup>23,24</sup> the primary fragmentation of styrene is

(23) Yu, C. F.; Youngs, F.; Bersohn, R.; Turro, N. J. *J. Phys. Chem.* **1985**, *89*, 4409.

(24) Dudek, D.; Glänzer, K.; Troe, J. *Ber. Bunsenges. Phys. Chem.* **1979**, *83*, 788.

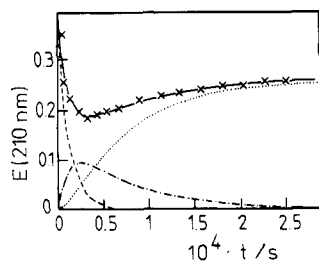


Figure 18. (—) Model calculation of the absorption-time profile in Figure 4 with contributions from styrene (---), benzene (.....), and benzene fragments (···) (×, experiment).

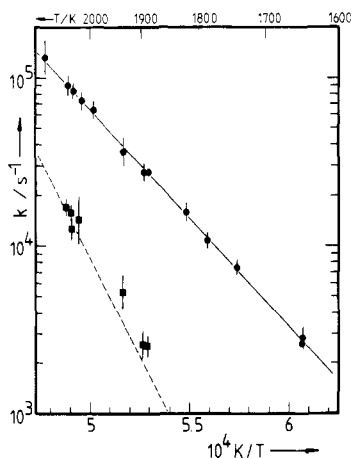
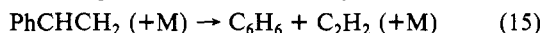
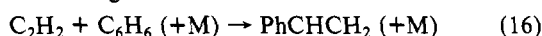


Figure 19. Rate coefficients for the unimolecular decomposition of styrene (●, —) and benzene (■) (in comparison with ref 26, ---); [Ar] =  $3.0 (\pm 0.5) \times 10^{-5} \text{ mol cm}^{-3}$ .

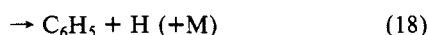
postulated to proceed via the isomerization into a bicyclic intermediate which is also accessible from the cyclooctatetraene side. This then breaks up into benzene and acetylene



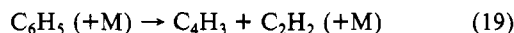
We simulated the observed profiles with a very simplified mechanism including the reverse of reaction 15



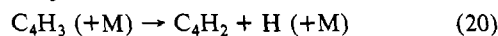
benzene fragmentation



and phenyl fragmentation



Further fragmentation of  $\text{C}_4\text{H}_3$  and benzene re-formation are also known to be of importance<sup>10,25</sup>



On the basis of reactions 15–19 and the styrene, benzene, and fragment spectra, we reproduced absorption time profiles very well as demonstrated in Figure 18. The simulations were sufficiently sensitive to allow the derivation of styrene and benzene decomposition rate constants  $k_{15}$  and  $k_{17} + k_{18}$ . The results are shown in Figure 19. The present data for benzene dissociation agree well with the results from ref 26, confirming the consistency of the treatment. The styrene dissociation rate constant

$$k_{15} = 10^{11.2 \pm 0.3} \exp(-244.5 \pm 12 \text{ kJ mol}^{-1} / RT) \text{ s}^{-1}$$

([Ar] =  $3 \times 10^{-5} \text{ mol cm}^{-3}$ , 1640–220 K) obviously corresponds to a complex dissociation reaction. We do not attempt, at this

(25) Kern, R. D.; Wu, C. H.; Skinner, G. B.; Rao, V. S.; Kiefer, J. H.; Towers, J. A.; Mizerka, L. J. *Symp. (Int.) Combust., (Proc.), 20th* 1984, 789.  
(26) Hsu, D. S. Y.; Lin, C. Y.; Lin, M. C. *Symp. (Int.) Combust., (Proc.), 20th* 1984, 626.

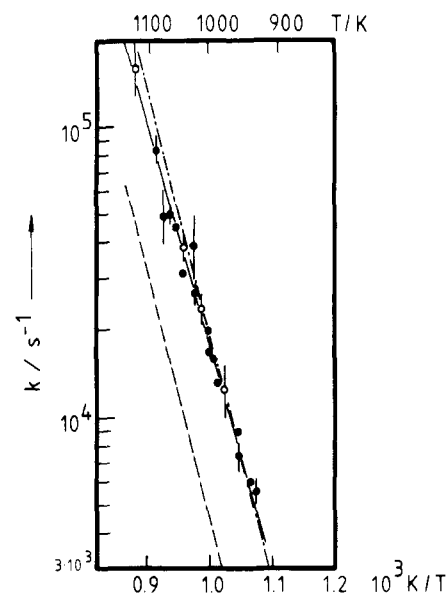


Figure 20. First-order rate coefficients for HBr elimination from 1-bromo-1-phenylethane (this work (●) incident shock, [Ar] =  $1.0 \times 10^{-5} \text{ mol cm}^{-3}$ ; (○) reflected shock, [Ar] =  $2.3 \times 10^{-5} \text{ mol cm}^{-3}$ ; (---) extrapolation from 520 to 560 K from ref 27, cited in ref 28; (.....) estimation from ref 28).

time, to interpret the detailed mechanism. However, the earlier remarks about the isomerization/hydrogen shift mechanism followed by  $\text{C}_2\text{H}_2$  elimination may explain the derived rate parameter. Independent verifications of our styrene experiments are desirable.

As a byproduct of our styrene studies, we have measured the HBr elimination from 1-bromo-1-phenylethane. There is a 1:1 conversion into styrene; no complications of the mechanism, being purely



were observed. Figure 20 shows the rate coefficients from incident and reflected shock waves. Our results are about a factor 3 higher than extrapolations from the limited low-temperature range 520–560 K investigated earlier.<sup>27,28</sup> The Arrhenius parameters of our results

$$k_{22} = 10^{12.5 \pm 0.2} \exp(-160 (\pm 10) \text{ kJ mol}^{-1} / RT) \text{ s}^{-1}$$

correspond well to a normal elimination reaction. They agree well with estimates from ref 28.

### Primary Products in Isopropylbenzene and *tert*-Butylbenzene Dissociation

The analysis of product spectra in our earlier investigations of isopropylbenzene and *tert*-butylbenzene pyrolysis<sup>4</sup> pointed in the direction of marked contributions from C–H bond splits. In the light of the new insight into benzyl radical spectra and kinetics, these experiments together with new results have to be reconsidered. Figure 7 showed the appearance of a product absorption, with a rate coefficient  $3.2 \times 10^4 \text{ s}^{-1}$  at 1660 K, which remained stable during the observation time. The identity of the product

(27) Stevenson, B. Ph.D. Thesis, London, 1957.

(28) Benson, S. W.; O'Neil, H. E. "Kinetic Data on Gas Phase Unimolecular Reactions"; *Natl. Stand. Ref. Data Ser. (U.S., Natl. Bur. Stand.)* 1970, No. 21.

(29) Brooks, C. T.; Peacock, S. J.; Reuben, B. R. *J. Chem. Soc., Faraday Trans. 1* 1982, 78, 3187.

(30) Litzinger, T. A.; Brezinsky, K.; Glassman, I. *Combust. Flame* 1986, 63, 251.

(31) Robaugh, D.; Tsang, W. *J. Phys. Chem.* 1986, 90, 4159.

(32) Stull, D. R.; Westrum, E. F.; Sinke, G. C. *The Chemical Thermodynamics of Organic Compounds*; Wiley: New York, 1969.

(33) Nakashima, N.; Yoshihara, K. *J. Chem. Phys.* 1983, 79, 2727.

(34) Brouwer, L.; Troe, J., unpublished results, 1981.

spectra in isopropyl and *tert*-butylbenzene pyrolysis in ref 4 was interpreted by the common product, in one case by C-H bond split, in the other by C-C bond split. Some of the arguments in favor of this interpretation do not apply any longer. Therefore, the stable end absorption of isopropylbenzene pyrolysis in Figure 6 can now equally well be interpreted by a primary C-C bond split followed by phenylethyl decomposition forming styrene, i.e.



The analogous C-C bond split in *tert*-butyl benzene with subsequent formation of  $\alpha$ -methylstyrene, i.e.



would lead to the product spectrum of  $\alpha$ -methylstyrene. Our present investigations of genuine  $\alpha$ -methylstyrene indicate very similar spectroscopic and kinetic properties of this molecule and styrene. Therefore, the identity of product spectra from isopropyl and *tert*-butylbenzene, as demonstrated in Figure 11, finds a rational explanation in terms of primary C-C bond splits as well. In our present work we have not attempted to analyze the details of the decomposition kinetics of these molecules. Various radical attacks of the parent molecules in analogy to the ethylbenzene mechanism are certainly important secondary processes following reactions 23 and 3, or 24 and 25. In this way, the high-temperature pyrolysis mechanisms soon become of similar or even larger complexity as for ethylbenzene and toluene. However, an

extensive formation of styrene and  $\alpha$ -methylstyrene, respectively, from our observations appears probable.

### Conclusions

The present work has demonstrated that UV molecular absorption spectroscopy, in spite of overlapping absorption continua from several species, can be used for analyzing the high-temperature pyrolysis of ethylbenzene. A dominant C-C bond split was identified and its rate constant was measured. Inspection of the complex mechanism of secondary reactions reconfirmed the surprisingly fast rate of consumption of benzyl radicals. The observations of benzyl radical properties, which we have verified now with several different benzyl precursors, call for a reinterpretation of several shock wave studies using other detection techniques. A clarification of the benzyl fragmentation pathways and rates may be expected from separate laser photolysis studies of benzyl radicals. The high-temperature pyrolysis mechanism of aromatic hydrocarbons apparently involves a much more complicated mechanism of secondary reactions, as compared to that at moderate temperature conditions, that intense future work is required before a complete modelling is possible.

*Acknowledgment.* Financial support of this work by the Deutsche Forschungsgemeinschaft as well as discussions of laser photolysis experiments with L. Lindemann are gratefully acknowledged.

**Registry No.** PhCH<sub>2</sub>CH<sub>3</sub>, 100-41-4; PhCHCH<sub>3</sub>, 2348-51-8; CH<sub>3</sub>, 2229-07-4; H, 12385-13-6; PhCH<sub>3</sub>, 108-88-3; PhCH<sub>2</sub>, 2154-56-5; PhCHBrCH<sub>3</sub>, 585-71-7; PhCH(CH<sub>3</sub>)<sub>2</sub>, 98-82-8; PhC(CH<sub>3</sub>)<sub>3</sub>, 98-06-6; styrene, 100-42-5; benzyl iodide, 620-05-3;  $\alpha$ -methylstyrene, 98-83-9.

## Photochemistry in Strongly Absorbing Media

James R. Sheats,\*

Hewlett-Packard Laboratories, 3500 Deer Creek Road, Palo Alto, California 94304

James J. Diamond,\* and Jonathan M. Smith†

Department of Chemistry, Bates College, Lewiston, Maine 04240 (Received: September 29, 1987; In Final Form: February 8, 1988)

We report the solution to the coupled nonlinear first-order partial differential equations representing the dynamics of photochemical reactions in systems essentially free from diffusion. No limitation regarding absorption of light by products or inert medium is assumed. These equations have been solved with the boundary condition that the species be uniformly distributed in the material prior to irradiation; the incident light may have an arbitrary time dependence. This analytical method of solution has been applied to photobleaching reactions described by various rate laws, where both reactants and products can absorb light. In addition, model systems in which the products absorb more than the reactants (photoantibleaching reactions) are also studied. An empirical procedure is introduced that accounts for changes in surface reflectance during the photoreaction in a satisfactory manner. Finally, a comparison is made with the corresponding equations describing photochemistry in perfectly stirred media.

### Introduction

Photochemical reactions in condensed media are of interest in a wide variety of applications; examples range from lithography for microcircuit fabrication<sup>1</sup> and optical data recording<sup>2-4</sup> to polymer degradation<sup>5,6</sup> and solar energy capture.<sup>7-10</sup> In such systems the resultant chemical transformation is often governed by a pair of coupled partial differential equations:

$$-\frac{\partial C_r(z,t)}{\partial t} = kIF(C_r) \quad (1)$$

$$-\frac{\partial I(z,t)}{\partial z} = (\alpha_r C_r + \alpha_p C_p + \alpha_m C_m)I \quad (2)$$

Here  $C_r$  denotes the concentrations of reactants,  $C_p$  that of products, and  $C_m$  that of an inert medium;  $\alpha_i$  the respective (base  $e$ ) molar extinction coefficients, and  $t$  and  $z$  refer to time and position (along the beam direction), respectively;  $I(z,t)$  represents

(1) Thompson, L. F.; Willson, C. G.; Bowden, M. J. *Introduction to Microlithography*; ACS Symposium Series 219; American Chemical Society: Washington, DC, 1983.

(2) Janai, M.; Moser, F. J. *J. Appl. Phys.* **1982**, *53*, 1385-1386.

(3) Morinaka, A.; Oikawa, S.; Yamazaki, H. *Appl. Phys. Lett.* **1983**, *43*, 524-526.

(4) Moerner, W. E.; Levenson, M. D. *J. Opt. Soc. B* **1985**, *2*, 915-924.

(5) Gooden, R.; Hellman, M. Y.; Hutton, R. S.; Winslow, F. H. *Macromolecules* **1984**, *17*, 2830-2837.

(6) Marinero, E. E. *Chem. Phys. Lett.* **1985**, *115*, 501-506.

(7) Renschler, C. L.; Faulkner, L. R. *J. Am. Chem. Soc.* **1982**, *104*, 3315-3320.

(8) Hargreaves, J. S.; Webber, S. E. *Macromolecules* **1982**, *15*, 424-429.

(9) Kim, N.; Webber, S. E. *Macromolecules* **1982**, *15*, 430-435.

(10) Ng, D.; Guillet, J. E. *Macromolecules* **1982**, *15*, 724-727.

† Current address: Department of Chemistry, Wesleyan University, Middletown, CT 06457.